



Published in final edited form as:

Hepatology. 2011 May ; 53(5): 1662–1675. doi:10.1002/hep.24253.

Paneth cell-derived IL-17A causes multi-organ dysfunction after hepatic ischemia and reperfusion injury

Sang Won Park¹, Mihwa Kim¹, Kevin M. Brown¹, Vivette D. D'Agati², and H. Thomas Lee^{1, #}

¹ Department of Anesthesiology, College of Physicians and Surgeons of Columbia University, New York, NY 10032

² Department of Pathology, College of Physicians and Surgeons of Columbia University, New York, NY 10032

Abstract

Hepatic ischemia and reperfusion (IR) injury is a major clinical problem that leads to frequent extra-hepatic complications including intestinal dysfunction and acute kidney injury (AKI). In this study, we aimed to determine the mechanisms of hepatic IR-induced extra-hepatic organ dysfunction. Mice subjected to 60 min of hepatic IR not only developed severe hepatic injury but also developed significant AKI and small intestinal injury. Hepatic IR induced small intestinal Paneth cell degranulation and increased IL-17A levels in portal vein plasma and small intestine. We also detected increased levels of IL-17A mRNA and protein in Paneth cells after hepatic IR with laser capture dissection. IL-17A neutralizing antibody treatment or genetic deletion of either IL-17A or IL-17A receptors significantly protected against hepatic IR-induced acute liver, kidney and intestinal injury. Leukocyte IL-17A does not contribute to organ injury as infusion of wild type splenocytes failed to exacerbate liver and kidney injury in IL-17A deficient mice after hepatic IR. Depletion of Paneth cell numbers by pharmacological (with dithizone) or genetic intervention (SOX9 flox/flox Villin cre+/- mice) significantly attenuated intestinal, hepatic, and renal injury following liver IR. Finally, depletion of Paneth cell numbers significantly decreased small intestinal IL-17A release and plasma IL-17A levels after liver IR. Taken together, the results show that Paneth cell derived IL-17A plays a critical role in hepatic IR injury and extra-hepatic organ dysfunction. Modulation of Paneth cell dysregulation may have therapeutic implications by reducing systemic complications arising from hepatic IR.

Keywords

apoptosis; dithizone; inflammation; kidney; liver; necrosis; small intestine

Introduction

Hepatic ischemia and reperfusion (IR) complicates liver transplantation and major liver resection (1). Furthermore, hepatic IR frequently leads to extra-hepatic organ injury including the kidney, intestine and lung (2). In particular, acute kidney injury (AKI) after major liver IR is extremely common (40–85% incidence) and the development of AKI after liver injury greatly increases patient mortality and morbidity during the perioperative period

[#]Address for Correspondence: H. Thomas Lee, M.D., Ph.D., Associate Professor, Department of Anesthesiology, Anesthesiology Research Laboratories, Columbia University, P&S Box 46 (PH-5), 630 West 168th Street, New York, NY 10032-3784, Tel: (212) 305-1807 (Lab), Fax: (212) 305-8980.

Disclosure

None of the authors had financial interests or ties to commercial companies.

(2). Furthermore, extra-hepatic manifestations of liver IR not only contribute significantly to remote organ (e.g., kidney, intestine) injury but also exacerbate hepatic IR injury. Unfortunately, the detailed mechanisms involved in extra-hepatic organ dysfunction due to hepatic IR remain obscure.

IL-17A is a pro-inflammatory cytokine released by T-cells as well as by innate immune cells and plays a critical role in both innate and adaptive immunity (3–6). Not surprisingly, IL-17A dysregulation has been implicated in several auto-immune diseases with heightened inflammatory responses in humans and in mice (3). In our previous studies, we showed that AKI leads to increased small intestinal IL-17A release and plasma IL-17A levels (7). Takahashi *et al.* recently demonstrated that small intestinal Paneth cells produce and release IL-17A to mediate TNF- α induced shock (4). Therefore, small intestinal Paneth cells may function as a reservoir of pro-inflammatory IL-17A and Paneth cell-derived IL-17A may potentiate liver injury, systemic inflammation and extra-hepatic organ dysfunction.

In this study, we tested the hypothesis that hepatic IR induces Paneth cell dysregulation, increased IL-17A production and release. A combination of pharmacological and genetic depletion approaches were used to determine the role of small intestinal Paneth cells as a source of IL-17A generation after hepatic IR resulting in exacerbation of liver injury and extra-hepatic (kidney and intestine) organ dysfunction.

Materials and Methods

Materials

Unless otherwise specified, all other reagents were purchased from Sigma (St. Louis, MO). Anti-(6C/A)-Crp1 antibody reactive against mouse alpha-defensin was a kind gift of Dr. Andre J. Ouellette (Keck School of Medicine of The University of Southern California, Los Angeles, CA).

Mice

All mice strains were bred or purchased on a C57BL/6 background. Male C57BL/6 mice (20–25 g) were obtained from Harlan, Indianapolis, IN. IL-17A deficient mice (IL-17A^{-/-}) were obtained as a gift from Yoichiro Iwakura (University of Tokyo, Tokyo, Japan) and IL-17A receptor deficient mice (IL-17R^{-/-}) were provided by Amgen Inc. Both IL-17A^{-/-} and IL-17R^{-/-} mice were congenic with C57BL/6 mice (8). Paneth cell deficient mice (SOX9 flox/flox Villin Cre^{+/-}) were generated as described and obtained from Yuko Mori-Akiyama (Baylor College of Medicine, Houston, TX) (9). SOX9 transcription factor is required for the differentiation of Paneth cells as intestinal inactivation of SOX9 resulted in mice with Paneth cell deficiency without affecting differentiation of other intestinal epithelial cell types (9). SOX9 flox/flox Villin Cre^{-/-} mice were used as wild type controls.

Induction of hepatic IR

All protocols were approved by the Institutional Animal Care and Use Committee of Columbia University. Male mice (20–25 g) were subjected to liver IR injury as described previously (10). This method of partial hepatic ischemia for 60 min. results in a segmental (~70%) hepatic ischemia but spares the right lobe of the liver and prevents mesenteric venous congestion by allowing portal decompression through the right and caudate lobes of the liver. Sham operated mice were subjected to laparotomy and identical liver manipulations without vascular occlusion. Five to 24 hrs after reperfusion, plasma, the liver, kidney and small intestine tissues were collected for analysis of tissue injury, inflammation, cytokine upregulation and apoptosis. We also collected systemic plasma 0.1, 1, 3, 5, 12 and 24 hrs after reperfusion to measure IL-17A levels with ELISA. To deplete Paneth cell

granules, mice were treated with dithizone (100 mg/kg, i.v.) 6 hrs prior hepatic ischemia as described (11,12). Dithizone (10 mg/ml) was dissolved in saturated lithium carbonate (1 g/100 mL). To neutralize IL-17A, mice were treated intravenously with 100 or 200 µg of anti-mouse IL-17A antibody (eBioscience, San Diego, CA) immediately before reperfusion. In order to determine whether leukocyte IL-17A contributes to hepatic IR injury and extra-hepatic organ dysfunction, spleens from wild-type (C57BL/6) mice were crushed and splenocytes were passed through a nylon cell strainer (BD Biosciences, San Jose, CA) and collected in phosphate-buffered saline. Red blood cells were lysed and single-cell splenocyte suspensions were transferred intravenously (6×10^6 to 1×10^7 splenocytes per transfer, 200 µl) to IL-17A^{-/-} mice 24 hrs before liver ischemia.

Measurement of plasma ALT activity and creatinine level

The plasma ALT activities were measured using the Infinity™ ALT assay kit according to the manufacturer's instructions (Thermo Fisher Scientific, Waltham, MA). Plasma creatinine was measured by an enzymatic creatinine reagent kit according to the manufacturer's instructions (Thermo Fisher Scientific, Waltham, MA). This method of creatinine measurement largely eliminates the interferences from mouse plasma chromagens well known to the Jaffe method (13).

Histological analysis of hepatic, small intestinal and renal injury

For histological preparations, liver, small intestine or kidney tissues were fixed in 10% formalin solution overnight. After automated dehydration through a graded alcohol series, tissues were embedded in paraffin, sectioned at 4 µm, and stained with hematoxylin-eosin (H&E). All H&E sections were evaluated for injury by a pathologist (VD'A) who was blinded to the treatment each animal had received. Liver H&E sections were graded for IR injury using the system devised by Suzuki *et al.* (14) and as described previously (10). In this classification, 3 liver injury indices - sinusoidal congestion (score: 0–4), hepatocyte necrosis (score: 0–4), and ballooning degeneration (score: 0–4) - are graded for a total score of 0–12. We also quantified percent liver necrotic area as well as degree of hepatocyte apoptosis after liver IR. Hepatic apoptosis was quantified by counting the number of apoptotic hepatocytes per high power field (400X) in necrotic and in non-necrotic (viable) zones. Total apoptosis score per liver section was estimated by multiplying the number of apoptotic cells in necrotic area by percent liver necrotic area. Intestine H&E sections were also blindly evaluated for intestinal epithelial cell necrosis, development of a necrotic pannus over the mucosal surface, villous endothelial cell apoptosis and swelling and blunting of villi because of villous mononuclear cell mucosal inflammation and edema. Renal H&E sections were evaluated for the severity (score: 0–3) of renal cortical vacuolization, peritubular/proximal tubule leukocyte infiltration, proximal tubule simplification and proximal tubule hypereosinophilia.

Enzyme Linked ImmunoSorbent Assay for IL-17A

Twenty four hrs after liver reperfusion, plasma, small intestine and isolated crypt IL-17A levels were measured with mouse specific IL-17A ELISA kit according to the manufacturer's instructions (eBiosciences, San Diego, CA). Tissues were homogenized in ice-cold RIPA buffer (150 mM NaCl, 50 mM Tris-HCl, 1 mM EDTA, and 1% Triton-X [pH 7.4]) and samples processed for mouse specific ELISA kits.

Cryptdin-1 immunoblotting

Small intestine tissues from SOX9 flox/flox Villin Cre^{+/-} (Paneth cell deficient) or SOX9 flox/flox Villin Cre^{-/-} (wild type control) mice were homogenized in ice-cold RIPA buffer (150 mM NaCl, 50 mM Tris-HCl, 1 mM EDTA, and 1% Triton-X [pH 7.4]) and processed

for cryptdin-1 immunoblotting with Anti-(6C/A)-Crp1 antibody as described previously (10,15).

Assessment of liver, small intestine and kidney inflammation

Liver, kidney and small intestine inflammation after hepatic ischemia was determined with detection of neutrophil infiltration by immunohistochemistry 24 hrs after hepatic IR as described previously (16) and by measuring mRNA encoding markers of inflammation, including keratinocyte derived cytokine (KC), intercellular adhesion molecule-1 (ICAM-1), monocyte chemoattractive protein-1 (MCP-1) and macrophage inflammatory protein-2 (MIP-2) 5 hrs after liver IR (Supplemental Table 1). Semi-quantitative real-time RT-PCR were performed as described (10).

Detection of liver, small intestine and kidney apoptosis

We used two additional independent assays to assess the degree of liver and intestine apoptosis 24 hrs after sham surgery or liver IR: *in situ* TUNEL assay and the detection of DNA laddering. For the TUNEL assay, formalin fixed sections were deparaffinized in xylene and rehydrated through graded ethanol to water. *In situ* TUNEL staining was used for detecting DNA fragmentation in apoptosis using a commercially available *in situ* cell death detection kit (Roche, Nutley, NJ) according to the manufacturer's instructions. For DNA laddering, apoptotic DNA fragments were extracted according to the methods of Herrmann *et al.* (17) and was electrophoresed at 70 V in a 2.0% agarose gelin Tris-acetate-EDTA buffer. This method of DNA extraction selectively isolates apoptotic, fragmented DNA and leaves behind the intact chromatin. The gel was stained with ethidium bromide and photographed under UV illumination. DNA ladder markers (100 bp) were added to a lane of each gel as a reference for the analysis of internucleosomal DNA fragmentation.

Isolation of intestinal crypts

Intact small intestinal crypts were isolated with the distended intestinal sac method as described by Traber *et al.* (18) with slight modifications. Small intestine (jejunum and ileum) was removed and rinsed thoroughly with intestinal wash solution [0.15 M NaCl, 1 mM dithiothreitol (DTT), and 40 pg/ml phenylmethylsulfonyl fluoride (PMSF)] and then filled with buffer A [(in mM) 96 NaCl, 27 sodium citrate, 1.5 KCl, 8 KH₂PO₄, 5.6 Na₂HPO₄, and 40 pg/ml PMSF (pH 7.4)]. The ends were clamped with micro-clips and the intestine was filled to a pressure of 50 cm H₂O. The filled intestine was submerged in oxygenated 0.15 M NaCl at 37°C for 40 min., drained and the solution was discarded. The intestine was then filled with buffer B [(in mM) 109 NaCl, 2.4 KCl, 1.5 KH₂PO₄, 4.3 Na₂HPO₄, 1.5 EDTA, 10 glucose, 5 glutamine, 0.5 DTT, and 40 pg/ml PMSF (pH 7.4)], incubated at 37°C for another 20 min. and the intestinal contents were drained and collected. The cells from 40–60 min. fraction containing intact and isolated crypts were collected by pelleting at 100 g for 5 min at 4°C and washed once with PBS.

Laser capture micro-dissection (LCM) of Paneth cells

LCM of individual Paneth cells was performed with the PixCell I LCM System (Arcturus Engineering, Mountain View, Calif., USA) as described (19). Small intestine tissues were excised and embedded in Optimum Cutting Temperature (OCT) compound (Sakura, Torrance, CA), sectioned at a thickness of 10 µm and mounted on 1.0 PEN Membrane Slides (Carl Zeiss, Thornwood, NY). The sections were then prepared for micro-dissection using an LCM staining kit (Ambion, Austin, Tx) through a graded alcohol series (95%, 75%, 50%) followed by cresyl violet staining. After de-staining via second graded alcohol series (50%, 75%, 95%), they were dehydrated in 100% ethanol followed by xylene. LCM was performed on a Zeiss Axiovert 200M microscope equipped with PALM RoboSoftware

(Carl Zeiss, Thornwood, NY) and the total area of tissue collected per slide was tracked and recorded. RNA was isolated from the dissected tissue by following the protocol provided by the RNAqueous-Micro kit (Ambion, Austin, TX) via column purification.

Electron Microscopy

Small intestines were fixed in 4% paraformaldehyde/3% glutaraldehyde in 10 mM sodium phosphate buffer (pH 7.4) for 48 hrs. All samples were postfixated with 1% osmium tetroxide in 100 mM cacodylate buffer (pH 7.4) on ice for 1 hr. Samples were then treated with 0.5% aqueous uranyl acetate, dehydrated in graded alcohol, treated with propylene oxide, and embedded in Embed 812 (Electron Microscopy Sciences). The resin was polymerized in a 60°C oven for 2–3 days. Sections were cut with a Dupont diamond knife in Reichert-Jung UltraCut E ultramicrotome, collected on copper grids, and doubly stained with saturated aqueous uranyl acetate and lead citrate. Ultrathin sections were imaged for Paneth cells using a JEM-1200EX electron microscope manufactured by JEOL.

Protein determination

Protein contents were determined with a bicinchoninic acid protein assay kit (Pierce Chemical Co., Rockford, IL), using bovine serum albumin as a standard.

Statistical analysis

All data are reported as mean \pm standard error. The overall significance of the results was examined using one-way analysis of variance and the significant differences between the groups were considered at a $P < 0.05$ with the appropriate Tukey's *post hoc* test made for multiple comparisons. The ordinal values of the liver and kidney injury scores were analyzed by the Mann-Whitney non-parametric test.

Results

Paneth cells degranulate after ischemic AKI or bilateral nephrectomy

Histological examination of small intestines from sham-operated mice showed Paneth cells containing densely packed eosinophilic secretory granules (Figure 1A). In contrast, after hepatic IR, rapid and extensive degranulation of Paneth cells was observed (magnification 400X, representative of 5 experiments, arrows and magnified insert) compared to sham-operated animals. Further evidence of Paneth cell degranulation was apparent by electron microscopy of small intestines following hepatic IR (Figure 1B). The crypt lumen from sham-operated mice was devoid of Paneth cell granules whereas the crypt lumen from mice subjected to hepatic IR showed granules being released into the lumen.

Increased IL-17A mRNA and protein in small intestinal crypt Paneth cells after hepatic IR

With laser capture micro-dissection, we selectively isolated Paneth cells to determine whether Paneth cells produce increased IL-17A mRNA 5 hrs after liver IR. mRNA recoveries were sufficient for performance of semi-quantitative RT-PCR for GAPDH and IL-17A which demonstrated increased IL-17A mRNA after bilateral nephrectomy (11 ± 1 fold over sham, $N=4$, $P < 0.01$, Figure 2). We also isolated intact small intestinal crypts containing Paneth cells 24 hrs after sham-operation or liver IR. Small intestinal crypts isolated with the distended sac method and stained with eosin-Y showed red staining characteristic of Paneth cells (Supplemental Figure 1). IL-17A ELISA performed in these isolated crypts showed that IL-17A protein levels were significantly increased (59 ± 4 pg/mg protein, $N=4$) compared to sham-operated mice (9 ± 3 pg/mg protein, $N=4$).

Hepatic IR increases plasma and tissue IL-17A production in mice

Wild type (C57BL/6) mice subjected to 60 min liver IR increased both systemic (Figure 3A) and portal venous (Figure 3B) IL-17A levels compared with the sham-operated mice (undetectable levels). The rise in systemic plasma was very rapid occurring within 1 hr after reperfusion. Moreover, the rise in portal venous levels of IL-17A was significantly greater ($P<0.05$) than the level detected in the systemic circulation. In addition, hepatic, renal and small intestine (jejunum) tissue IL-17A levels all increased ($P<0.01$) after hepatic IR compared to IL-17A levels detected in sham-operated mice liver, kidney and small intestine (Figure 3C). Consistent with higher portal venous IL-17A levels, small intestine IL-17A levels after liver IR were greater than the levels determined from the liver or kidney ($P<0.01$).

IL-17A plays a critical role in hepatic, renal and intestine injury after hepatic IR in mice

Mice subjected to liver IR not only developed severe liver dysfunction with significantly higher plasma ALT levels ($P<0.0001$ compared to sham-operated mice) but also developed AKI with significant rises in plasma Cr ($P<0.01$ vs. sham-operated mice) 24 hrs after hepatic ischemic injury (Figure 3D). Induction of IL-17A plays a critical role in generating hepatic and renal injury after liver IR as mice treated with IL-17A neutralizing antibody were significantly and dose-dependently protected against hepatic and renal injury after liver IR. In addition, mice deficient in IL-17A receptor or IL-17A were protected against hepatic and renal injury after liver IR. Furthermore, transfusion of IL-17A wild type splenocytes failed to exacerbate hepatic or renal injury in IL-17A deficient mice after liver IR suggesting that IL-17A from non-leukocyte source contributes to hepatic and renal injury. Plasma (systemic and portal vein) and tissue (liver, kidney and jejunum) levels of IL-17A were significantly reduced in mice treated with IL-17A antibody, in IL-17A receptor or IL-17A deficient mice (Figure 3A, 3B and 3C) after liver IR. We determined in pilot experiments that transfusion of IL-17A wild type splenocytes to IL-17A wild type mice did increase plasma and tissue IL-17A levels or alter renal or hepatic injury after liver IR (data not shown). Importantly, we were able to detect IL-17A protein expression plasma (Figure 3A and 3B) and tissues (Figure 3C) of IL-17A deficient mice transfused with IL-17A wild type splenocytes 24 hrs after hepatic IR. We also detected IL-17A mRNA expression in the kidney, liver and intestine of IL-17A deficient mice transfused with IL-17A wild type splenocytes (data not shown).

Representative H&E slides (magnification, 40X) of liver tissues from mice subjected to 60 min ischemia and 24 hrs reperfusion or to sham-operation are shown in Figure 4A. Sixty min of partial hepatic IR in wild type mice produced large necrotic areas after reperfusion (average percent necrotic area = $92\pm 2\%$, $N=6$). Livers were also analyzed for the degree of hepatocellular damage using the Suzuki's criteria (14). The ischemic lobes in the control group showed severe hepatocyte vacuolization, necrosis and sinusoidal congestion (Suzuki score= 9.4 ± 0.3 , $N=6$, Figure 4B). Neutralization of IL-17A (200 μg antibody), deficiency in IL-17A receptor or IL-17A significantly reduced liver necrosis and lowered Suzuki liver injury scores (Figure 4B). Moreover, transfusion of IL-17A wild type splenocytes failed to exacerbate liver necrosis in IL-17A deficient mice after liver IR.

Representative H&E slides from kidneys from mice subjected to 60 min liver ischemia and 24 hrs reperfusion are shown in Figure 5A (magnification 200X). Kidneys from the wild type mice subjected to liver IR demonstrated multi-focal acute tubular injury including S3 segment proximal tubule necrosis, cortical tubular simplification, cytoplasmic vacuolization and dilated lumina as well as focal granular bile/heme casts (Figure 5A). The summary of renal injury scores for percent renal tubular hypereosinophilia, percent peritubular leukocyte margination and percent cortical vacuolization are shown in Figure 5B. Neutralization of

IL-17A (200 µg antibody), deficiency in IL-17A receptor or IL-17A significantly reduced kidney injury. Consistent with plasma creatinine, IL-17A deficient mice transfused with IL-17A wild type splenocytes were still protected against kidney injury after liver IR.

Hepatic IR injury also caused severe small intestinal injury (Figure 6). Small intestine histology assessed 24 hrs after 60 min. hepatic IR in H&E stained sections demonstrated villous endothelial cell apoptosis (Figure 6B, magnified insert), villous epithelial cell necrosis and the development of a necrotic epithelial pannus over the mucosal surface. Neutralization of IL-17A (200 µg antibody, Figure 6C), deficiency in IL-17A (Figure 6D) or IL-17A receptor (Figure 6E) significantly reduced small intestine injury 24 hr after 60 min. hepatic IR. In addition, infusion of wild type splenocytes into IL-17A deficient mice did not reverse the intestinal protection in these mice (Figure 6F).

IL-17A blockade or deficiency reduces hepatic, renal and intestine inflammation and apoptosis after liver IR

We assessed tissue inflammation by detecting neutrophil infiltration and by measuring pro-inflammatory mRNA upregulation. Sixty min. of hepatic ischemia resulted in significant recruitment of neutrophils into the liver, kidney and intestine in IL-17A wild type mice (Supplemental Figures 2A–C). Neutrophil infiltration coincided with areas of liver necrosis. Neutralization of IL-17A, deficiency in IL-17A receptor or IL-17A significantly reduced neutrophil infiltration in all 3 organs.

We also measured the expression of pro-inflammatory cytokine mRNAs in the liver, kidney and intestine 24 hrs after liver IR with semi-quantitative RT-PCR. Hepatic IR significantly increased pro-inflammatory mRNA expression (ICAM-1, KC, MCP-1 and MIP-2) in all 3 organs compared to the sham-operated mice (Supplemental Figures 3A–C). However, Neutralization of IL-17A, deficiency in IL-17A receptor or IL-17A significantly reduced pro-inflammatory mRNA expression in all 3 organs. We were able to detect IL-17A mRNA expression in all tissues (data not shown) of IL-17A deficient mice transfused with IL-17A wild type splenocytes. Furthermore, wild type IL-17A splenocyte transfused IL-17A deficient mice showed significantly attenuated pro-inflammatory mRNA expression in the liver, kidney and small intestine (data not shown).

We utilized 3 separate indices to detect apoptosis: 1) TUNEL staining (Supplemental Figure 4), 2) DNA laddering (Supplemental Figure 5) and 3) counting the number of apoptotic hepatocytes in high power field (400X) H&E images (Supplemental Figure 6). Hepatic IR caused massive hepatocyte apoptosis. Moreover, we determined that apoptotic hepatocytes can be detected in both necrotic and non-necrotic areas after IR with significantly higher number of apoptotic cells in the necrotic zones of the liver. After hepatic IR, kidney and small intestine also showed severe capillary endothelial apoptosis (insert expanded in Supplemental Figures 4B and C). Neutralization of IL-17A, deficiency in IL-17A receptor or IL-17A significantly reduced apoptosis in all 3 organs (Supplemental Figures 4–6).

Pharmacological depletion of Paneth cells attenuates hepatic, renal and intestine injury after hepatic IR

Zinc depletion with dithizone treatment selectively and rapidly (with 1 hr) results in the loss of Paneth cell secretory granules in mice (11,12). Accordingly, we treated mice with dithizone to deplete Paneth cell granules to test the effect of this pharmacological ablation on the response to hepatic IR injury. Secretory granules are evident and abundant in ileal Paneth cells from vehicle (lithium carbonate)-treated mice (Figure 7A, left panel, arrows). In contrast, dithizone administration to mice almost completely depleted ileal Paneth cells of their granules within 6 h of dithizone exposure (Figure 7A, right panel, *).

We also stained small intestine crypts with lysozyme specific antibody as a marker of Paneth cell depletion after dithizone-treatment. We demonstrate that Paneth cell granule depletion with dithizone-treatment reduced lysozyme staining in small intestinal crypts after bilateral nephrectomy (Figure 7B). Note that lysozyme staining was heavy in Paneth cells (arrows) of small intestinal crypts of mice treated with vehicle (Li_2CO_3). Paneth cell depletion with dithizone treatment eliminated lysozyme staining in Paneth cells (*).

Treatment of Paneth cells with dithizone resulted in an approximately 64% reduction in plasma IL-17A levels 24 hrs after liver IR (Figure 7C). Furthermore, dithizone granule depletion drastically reduced IL-17A protein levels in the liver (76%), kidney (51%) and small intestine (67%) 24 hrs after liver IR (Figure 7C). Notably, Paneth cell depletion with dithizone caused greatest reduction in IL-17A levels in isolated crypts after liver IR to near sham-operated values (Figure 7C). Dithizone alone did not significantly affect IL-17A levels in sham-operated mice (data not shown).

Depletion of Paneth cell granules with dithizone improved liver and kidney function after 60 min of liver ischemia and 24 hr of reperfusion (Figure 7C). We also determined that Paneth cell granule depletion with dithizone significantly attenuated renal, hepatic and intestinal apoptosis (Supplemental Figures 5–7) and neutrophil infiltration (Supplemental Figures 8) after liver IR. In small intestine, we show that apoptotic cells are localized primarily to the tops of the villi and that dithizone treatment reduced intestinal apoptosis. Dithizone treatment did not induce Paneth cell or intestinal crypt apoptosis (Supplemental Figure 7C).

Mice genetically deficient for Paneth cells are protected against hepatic, renal and intestine injury after hepatic IR

To confirm that Paneth cell secretory products are required for hepatic, renal and intestinal injury induced by liver IR, we investigated the responses in mice genetically deficient in the Paneth cell lineage. We first confirmed that intestine specific SOX9-null (SOX9 flox/flox Villin Cre+/-) mice were deficient in Paneth cells by performing RT-PCR and immunoblotting for detection of the mouse Paneth cell α -defensin cryptdin-1, a Paneth cell specific marker. Intestine specific SOX9-null mice have significantly reduced cryptdin-1 mRNA and cryptdin-1 protein (Figure 8A), and H&E staining confirmed absent Paneth cell secretory granules in these intestine specific SOX9-null mice (Figure 8B), confirming stable genetic ablation of the lineage.

Intestine specific SOX9-null mice subjected to liver IR had significantly reduced IL-17A protein levels in plasma (~40%) and in the liver (~34%), kidney (~52%) and small intestine (~33%) 24 hrs after liver IR (Figure 8C). However, we demonstrate that Paneth cell deficiency in intestine specific SOX9-null mice reduced IL-17A protein levels in isolated crypts to near sham levels when compared to the wild type mice after liver IR (Figure 8C). Furthermore, Paneth cell deficient intestine specific SOX9-null mice were protected against hepatic and renal injury after 24 hrs after liver IR (Figure 8D) as measured by reduced plasma ALT and creatinine.

Discussion

We hypothesized that small intestinal Paneth cell-derived IL-17A plays a critical role in generating liver, kidney and intestine injury after hepatic IR. Our results support this hypothesis as 1) small intestinal Paneth cells degranulate and increase IL-17A production after liver IR, 2) plasma and tissue levels of IL-17A increase significantly with the highest IL-17A levels detected in portal vein plasma and in the small intestine, 3) depletion of IL-17A with neutralizing antibody or genetic deletion of either IL-17A or the IL-17A receptor protected against liver IR injury and extra-hepatic organ dysfunction, 4)

pharmacological (with dithizone treatment) or genetic depletion (with intestine specific SOX9 deletion) of Paneth cells attenuated hepatic, renal and intestinal injury following hepatic IR and 5) depletion of Paneth cell granules markedly decreased small intestinal IL-17A release and significantly attenuated plasma and tissue IL-17A levels after hepatic IR.

Hepatic IR injury is a common and unavoidable clinical complication in many major surgical procedures involving prolonged occlusion of the portal vein, inferior vena cava or aorta. Furthermore, hepatic IR injury frequently leads to extra-hepatic multi-organ dysfunction making therapeutic interventions extremely difficult (10,20). For example, patients subjected to hepatic IR frequently suffer from renal, respiratory and intestinal failure which drastically increases mortality, morbidity and prolongs ICU care. Initiation of remote organ injury in patients after liver IR further exacerbates liver injury creating a vicious cascade of multi-organ derangements. Therefore, a better understanding of the mechanisms of hepatic IR injury and extra-hepatic organ dysfunction would lead to improved therapy for patients subjected to unavoidable hepatic IR during the peri-operative period. However, the detailed mechanisms involved in extra-hepatic organ dysfunction due to hepatic IR are not fully elucidated. Studies to date implicate a complex orchestration of necrosis, apoptosis and inflammation mediated by hepatic (hepatocytes, Kupffer cells) and extra-hepatic (leukocytes, circulating cytokines) components (1,21).

We show that hepatic IR resulted in severe small intestinal injury as evidenced by villous endothelial apoptosis and villous epithelial necrosis (Figure 6). Small intestine has been implicated as a source of systemic inflammation, bacterial translocation and infection contributing significantly in multi-organ failure of critically ill patients (22,23). Furthermore, small intestine has been implicated in generating hepatocellular dysfunction in trauma or hemorrhagic shock as the injurious factors derived from the intestine attacks the liver first (22). Our results show that the concentration of IL-17A was highest in small intestine and in portal vein plasma (Figure 3).

We propose that hepatic IR upregulates small intestinal Paneth cell IL-17A production and Paneth cell-derived IL-17A plays an important role in propagating multi-organ injury after hepatic IR. We demonstrate rapid degranulation of small intestinal Paneth cells with induction of IL-17A after liver IR. Small intestinal Paneth cells are crucial for both mucosal as well as innate immunity against pathogens and can actively secrete several anti-microbial peptides (e.g., lysozyme, α -defensins/cryptdins) as well as pro-inflammatory molecules (e.g., inducible NO synthase, phospholipase A₂, IL-17A) (4,12,24–27). Therefore, although the Paneth cells (with the ability to kill bacteria and release pro-inflammatory mediators) are essential barriers providing mucosal and innate immunity (28,29), their dysregulation and overproduction of IL-17A after hepatic IR may lead to a systemic inflammatory syndrome and exacerbation of hepatic, intestinal and renal injury. It is likely that Paneth cell-derived IL-17A resulted in small intestinal inflammation and the influx of pro-inflammatory leukocytes with subsequent small intestinal tissue destruction and barrier disruption. Draining of pro-inflammatory mediators to the liver would then lead to exacerbation of hepatic IR injury.

Since freshly isolated individual crypts are free of leukocytes as well as cells of myeloid origin, we can rule out the contribution of leukocyte and myeloid source of increased IL-17A mRNA and protein after liver IR. However, since isolated crypts also contain stem cells and transit amplifying cells in addition to Paneth cells, we also performed LCM to specifically capture Paneth cells. We again confirmed increased expression of IL-17A mRNA in these Paneth cells captured by LCM (Figure 2). Furthermore, we demonstrate in this study that IL-17A generated from leukocytes do not contribute to hepatic IR injury and AKI as IL-17A deficient mice transfused with wild type splenocytes were still protected

against liver and kidney injury. Collectively, these data suggest that Paneth cell-derived IL-17A is responsible for generating intestinal, renal and hepatic injury after liver IR.

IL-17A is an important regulator of both innate and adaptive immunity and plays a critical role in host immune defense and inflammation (3,4). IL-17A production was originally characterized from Th17 cells of the CD4+ T cell subset distinct from Th1 or Th2 cells (5,6,30,31). Subsequent studies showed that other cell types including CD3+ natural killer T- cells, myeloid cells, neutrophils as well as Paneth cells can produce IL-17A in response to various inflammatory and pathogenic stimuli (3,4). Therefore, it is not surprising that IL-17A acts on various cell types, including neutrophils, endothelial cells and renal proximal tubule epithelial cells, inducing the expression of pro-inflammatory mediators such as IL-8, IL-6 and CXCL chemokines (32). Interestingly, the intestinal lamina propria was shown to be a unique site for detectable IL-17A levels in naive animals (8). Atarashi *et al.* confirmed these findings and demonstrated high amounts of IL-17A producing Th17 cells in the intestinal lamina propria but not in the spleen, mesenteric lymph nodes or Peyer's patches of a healthy mouse (33). Recently, Takahashi *et al.* showed that IL-17A produced by intestinal Paneth cells drive TNF- α induced inflammation and shock (4). These previous and our current studies suggest that Paneth cell dysregulation and IL-17A release plays a major role in multi-organ dysfunction and inflammation.

Pharmacological or genetic Paneth cell granule depletion attenuated hepatic, intestinal and renal injury and reduced tissue and plasma IL-17A levels after liver IR. We depleted Paneth cell granules with dithizone, a zinc chelator, as Paneth cell granule formation requires zinc (11,12). Although our TUNEL data (Supplemental Figure 7C) demonstrate that dithizone did not induce small intestinal Paneth cell apoptosis, use of dithizone may be limited by systemic side effects (e.g., pulmonary toxicity) at high doses and Paneth cell depletion is transient (with complete re-population of Paneth cells at 12–24 hrs after injection). Therefore, we complemented the dithizone studies with studies in intestine specific SOX9-null mice. Wnt, the Wnt Frizzled-5 receptor, Math1, Gfi1, and SOX9 are required for the development of Paneth cells (9,34). SOX9/Villin Cre $^{+/-}$ mice lack SOX9 transcription factor in intestinal epithelia and as a result show absent or significantly reduced numbers of mature Paneth cells in adult mice (9). These 2 approaches of Paneth cell depletion allowed us to conclude that Paneth cells are critical in generating extra-hepatic intestinal and renal injury after liver IR. However, Paneth cell depleted mice still had significant degree of hepatocyte necrosis (and elevated plasma ALT) due to prolonged liver ischemia (Figure 7D and Figure 8D). These findings suggest that both Paneth cell independent (hepatocyte necrosis) and Paneth cell dependent extra-hepatic injury contribute to hepatic IR injury *in vivo*.

With pharmacological or genetic Paneth cell granule depletion, we observed a striking reduction in IL-17A upregulation in isolated crypts with profound hepatic, intestinal and renal protection after liver IR. Although significantly attenuated, plasma and tissue IL-17A levels in Paneth cell depleted mice (Figure 7 and Figure 8) subjected to liver IR were still elevated compared to sham-operated mice. It is likely that several cell types including leukocytes and epithelial cells can generate IL-17A in response to liver IR and oxidant stress during reperfusion (3,6).

The mechanisms leading to Paneth cell degranulation and increased Paneth cell-derived IL-17A after hepatic IR remain to be determined. Our model of hepatic IR with partial portal vein and artery occlusion avoids total intestinal outflow obstruction. However, intestinal venous congestion with resultant partial intestinal ischemia may occur as 100% of intestinal blood flow is diverted to ~30% of hepatic mass. Partial intestinal IR may have contributed to Paneth cell degranulation and dysregulation. In addition, hepatic IR releases endogenous

Damage associated molecular pattern molecules (DAMPs including endotoxin, HMGB-1, mitochondrial DNA, uric acid) that can activate several toll-like receptors (TLRs) (35). TLR-mediated Paneth cell degranulation has been described (36,37).

In summary, we show that neutralization or genetic deletion of IL-17A provides powerful multi-organ protection after liver IR. In addition, we demonstrated that small intestinal Paneth cells degranulate to play a critical role in hepatic, intestinal and renal injury after liver IR. In addition, Paneth cells are a major initial source of IL-17A production after hepatic IR. We propose that the small intestinal Paneth cell generation of IL-17A leads to hepatic injury and extra-hepatic organ dysfunction. Modulation of Paneth cell dysregulation may have important therapeutic implications in reducing systemic complications arising from hepatic IR injury.

Supplementary Material

Refer to Web version on PubMed Central for supplementary material.

Acknowledgments

This work was supported by Department of Anesthesiology, Columbia University and by National Institute of Health Grants RO1 DK-58547 and RO1 GM-067081.

We would like to thank Dr. Andre J. Ouellette (Keck School of Medicine of The University of Southern California, Los Angeles, CA) for providing us with mouse alpha-defensin antibody and Dr. Yuko Mori-Akiyama (Baylor College of Medicine, Houston, TX) for sending us breeder pairs of intestine-specific SOX9 null mice.

References

1. Kupiec-Weglinski JW, Busuttill RW. Ischemia and reperfusion injury in liver transplantation. *Transplant Proc.* 2005 May; 37(4):1653–1656. [PubMed: 15919422]
2. Davis CL, Gonwa TA, Wilkinson AH. Pathophysiology of renal disease associated with liver disorders: implications for liver transplantation. Part I. *Liver Transpl.* 2002 Feb; 8(2):91–109. [PubMed: 11862584]
3. Cua DJ, Tato CM. Innate IL-17-producing cells: the sentinels of the immune system. *Nat Rev Immunol.* 2010 Jul; 10(7):479–489. [PubMed: 20559326]
4. Takahashi N, Vanlaere I, de RR, Cauwels A, Joosten LA, Lubberts E, et al. IL-17 produced by Paneth cells drives TNF-induced shock. *J Exp Med.* 2008 Aug 4; 205(8):1755–1761. [PubMed: 18663129]
5. Chang SH, Dong C. IL-17F: regulation, signaling and function in inflammation. *Cytokine.* 2009 Apr; 46(1):7–11. [PubMed: 19233684]
6. Gaffen SL, Kramer JM, Yu JJ, Shen F. The IL-17 cytokine family. *Vitam Horm.* 2006; 74:255–282. [PubMed: 17027518]
7. Park SW, Chen SW, Kim M, Brown KM, Kolls JK, D'Agati VD, et al. Cytokines induce small intestine and liver injury after renal ischemia or nephrectomy. *Lab Invest.* 2010 In Press.
8. Ivanov II, McKenzie BS, Zhou L, Tadokoro CE, Lepelley A, Lafaille JJ, et al. The orphan nuclear receptor ROR γ directs the differentiation program of proinflammatory IL-17+ T helper cells. *Cell.* 2006 Sep 22; 126(6):1121–1133. [PubMed: 16990136]
9. Mori-Akiyama Y, van den BM, van Es JH, Hamilton SR, Adams HP, Zhang J, et al. SOX9 is required for the differentiation of paneth cells in the intestinal epithelium. *Gastroenterology.* 2007 Aug; 133(2):539–546. [PubMed: 17681175]
10. Lee HT, Park SW, Kim M, D'Agati VD. Acute kidney injury after hepatic ischemia and reperfusion injury in mice. *Lab Invest.* 2009 Feb 1; 89(2):196–208. [PubMed: 19079326]
11. Sawada M, Takahashi K, Sawada S, Midorikawa O. Selective killing of Paneth cells by intravenous administration of dithizone in rats. *Int J Exp Pathol.* 1991 Aug; 72(4):407–421. [PubMed: 1883741]

12. Seno H, Sawada M, Fukuzawa H, Morita-Fujisawa Y, Takaishi S, Hiai H, et al. Involvement of tumor necrosis factor alpha in intestinal epithelial cell proliferation following Paneth cell destruction. *Scand J Gastroenterol.* 2002 Feb; 37(2):154–160. [PubMed: 11843050]
13. SLOT C. Plasma creatinine determination. A new and specific Jaffe reaction method. *Scand J Clin Lab Invest.* 1965; 17(4):381–387. [PubMed: 5838275]
14. Suzuki S, Toledo-Pereyra LH, Rodriguez FJ, Cejalvo D. Neutrophil infiltration as an important factor in liver ischemia and reperfusion injury. Modulating effects of FK506 and cyclosporine. *Transplantation.* 1993 Jun; 55(6):1265–1272. [PubMed: 7685932]
15. Lee HT, Kim M, Jan M, Penn RB, Emala CW. Renal tubule necrosis and apoptosis modulation by A1 adenosine receptor expression. *Kidney Int.* 2007 Apr 11; 71(12):1249–1261. [PubMed: 17429344]
16. Kim J, Kim M, Song JH, Lee HT. Endogenous A1 adenosine receptors protect against hepatic ischemia reperfusion injury in mice. *Liver Transpl.* 2008 Jun; 14(6):845–854. [PubMed: 18324658]
17. Herrmann M, Lorenz HM, Voll R, Grunke M, Woith W, Kalden JR. A rapid and simple method for the isolation of apoptotic DNA fragments. *Nucleic Acids Res.* 1994 Dec 11; 22(24):5506–5507. [PubMed: 7816645]
18. Traber PG, Gumucio DL, Wang W. Isolation of intestinal epithelial cells for the study of differential gene expression along the crypt-villus axis. *Am J Physiol.* 1991 Jun; 260(6 Pt 1):G895–G903. [PubMed: 2058677]
19. Tanji N, Ross MD, Cara A, Markowitz GS, Klotman PE, D'Agati VD. Effect of tissue processing on the ability to recover nucleic acid from specific renal tissue compartments by laser capture microdissection. *Exp Nephrol.* 2001; 9(3):229–234. [PubMed: 11340308]
20. Fondevila C, Busutil RW, Kupiec-Weglinski JW. Hepatic ischemia/reperfusion injury--a fresh look. *Exp Mol Pathol.* 2003 Apr; 74(2):86–93. [PubMed: 12710939]
21. Serracino-Inglott F, Habib NA, Mathie RT. Hepatic ischemia-reperfusion injury. *Am J Surg.* 2001 Feb; 181(2):160–166. [PubMed: 11425059]
22. Wang P, Ba ZF, Cioffi WG, Bland KI, Chaudry IH. Is gut the “motor” for producing hepatocellular dysfunction after trauma and hemorrhagic shock? *J Surg Res.* 1998 Feb 1; 74(2):141–148. [PubMed: 9587352]
23. Koo DJ, Zhou M, Jackman D, Cioffi WG, Bland KI, Chaudry IH, et al. Is gut the major source of proinflammatory cytokine release during polymicrobial sepsis? *Biochim Biophys Acta.* 1999 Aug 30; 1454(3):289–295. [PubMed: 10452963]
24. Huttner KM, Selsted ME, Ouellette AJ. Structure and diversity of the murine cryptdin gene family. *Genomics.* 1994 Feb; 19(3):448–453. [PubMed: 8188287]
25. Ouellette AJ, Hsieh MM, Nosek MT, Cano-Gauci DF, Huttner KM, Buick RN, et al. Mouse Paneth cell defensins: primary structures and antibacterial activities of numerous cryptdin isoforms. *Infect Immun.* 1994 Nov; 62(11):5040–5047. [PubMed: 7927786]
26. Ouellette AJ. Paneth cell alpha-defensin synthesis and function. *Curr Top Microbiol Immunol.* 2006; 306:1–25. [PubMed: 16909916]
27. Bultinck J, Sips P, Vakaet L, Brouckaert P, Cauwels A. Systemic NO production during (septic) shock depends on parenchymal and not on hematopoietic cells: in vivo iNOS expression pattern in (septic) shock. *FASEB J.* 2006 Nov; 20(13):2363–2365. [PubMed: 17020927]
28. Ouellette AJ. Paneth cell alpha-defensins: peptide mediators of innate immunity in the small intestine. *Springer Semin Immunopathol.* 2005 Sep; 27(2):133–146. [PubMed: 15931529]
29. Ouellette AJ. Defensin-mediated innate immunity in the small intestine. *Best Pract Res Clin Gastroenterol.* 2004 Apr; 18(2):405–419. [PubMed: 15123078]
30. Kramer JM, Hanel W, Shen F, Isik N, Malone JP, Maitra A, et al. Cutting edge: identification of a pre-ligand assembly domain (PLAD) and ligand binding site in the IL-17 receptor. *J Immunol.* 2007 Nov 15; 179(10):6379–6383. [PubMed: 17982023]
31. Nakae S, Komiyama Y, Nambu A, Sudo K, Iwase M, Homma I, et al. Antigen-specific T cell sensitization is impaired in IL-17-deficient mice, causing suppression of allergic cellular and humoral responses. *Immunity.* 2002 Sep; 17(3):375–387. [PubMed: 12354389]

32. Weaver CT, Hatton RD, Mangan PR, Harrington LE. IL-17 family cytokines and the expanding diversity of effector T cell lineages. *Annu Rev Immunol.* 2007; 25:821–852. [PubMed: 17201677]
33. Atarashi K, Nishimura J, Shima T, Umesaki Y, Yamamoto M, Onoue M, et al. ATP drives lamina propria T(H)17 cell differentiation. *Nature.* 2008 Oct 9; 455(7214):808–812. [PubMed: 18716618]
34. Bastide P, Darido C, Pannequin J, Kist R, Robine S, Marty-Double C, et al. Sox9 regulates cell proliferation and is required for Paneth cell differentiation in the intestinal epithelium. *J Cell Biol.* 2007 Aug 13; 178(4):635–648. [PubMed: 17698607]
35. Arumugam TV, Okun E, Tang SC, Thundiyil J, Taylor SM, Woodruff TM. Toll-like receptors in ischemia-reperfusion injury. *Shock.* 2009 Jul; 32(1):4–16. [PubMed: 19008778]
36. Foureau DM, Mielcarz DW, Menard LC, Schulthess J, Werts C, Vasseur V, et al. TLR9-dependent induction of intestinal alpha-defensins by *Toxoplasma gondii*. *J Immunol.* 2010 Jun 15; 184(12):7022–7029. [PubMed: 20488791]
37. Rumio C, Besusso D, Palazzo M, Selleri S, Sfondrini L, Dubini F, et al. Degranulation of paneth cells via toll-like receptor 9. *Am J Pathol.* 2004 Aug; 165(2):373–381. [PubMed: 15277213]

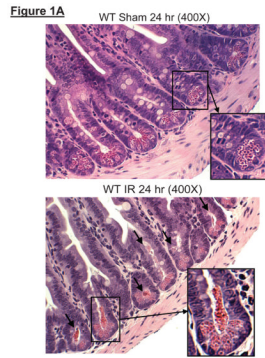


Figure 1B

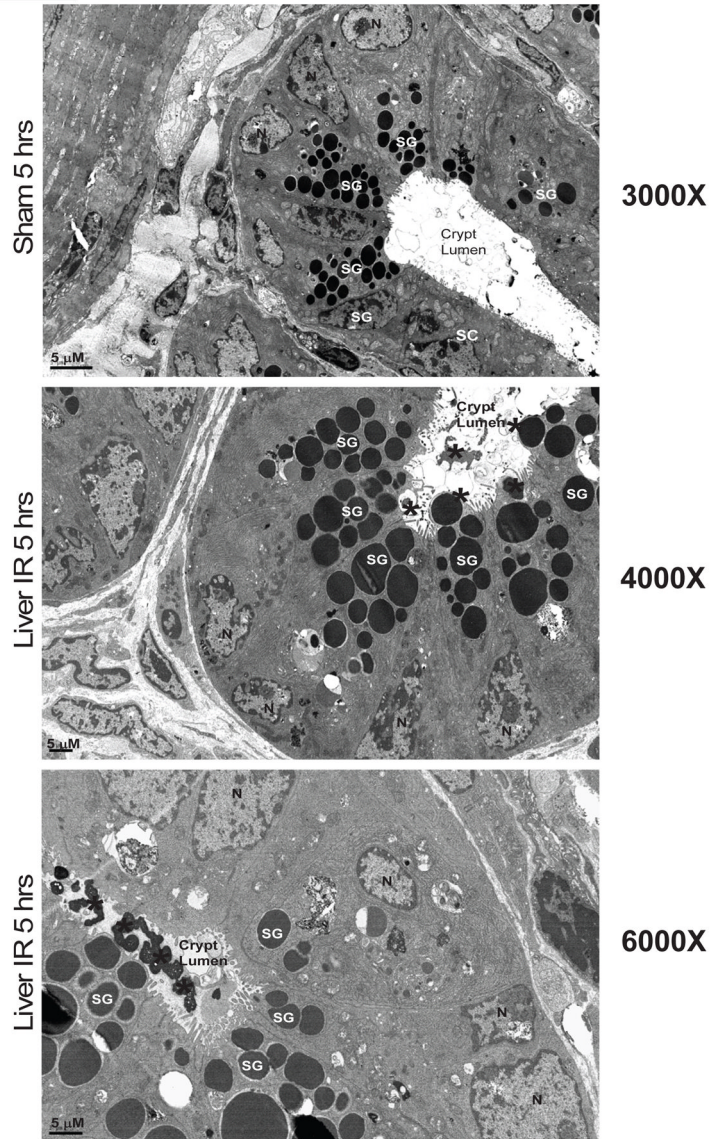


Figure 1.
 A. Representative H&E staining images of small intestinal (ileum shown) Paneth cells containing dense eosinophilic granules within their apical cytoplasm (400X magnification).

Hepatic IR resulted in small intestinal Paneth cell degranulation (B and C) in 5 hrs compared to sham-operated animals (A). Inserts show enlarged images of Paneth cells showing degranulation into the crypt lumen. Representative of 5 experiments. B. Representative electron micrograph images of small intestinal Paneth cell degranulation (indicated by *) 5 hrs after hepatic IR (4000X and 6000X magnification shown) compared to sham-operated mice (3000X magnification). The crypt lumen from sham-operated mice was devoid of Paneth cell granules. Representative of 3 experiments. N = nucleus of Paneth cells. SG = secretory granules of Paneth cells. SC = stem cells located above the Paneth cells.

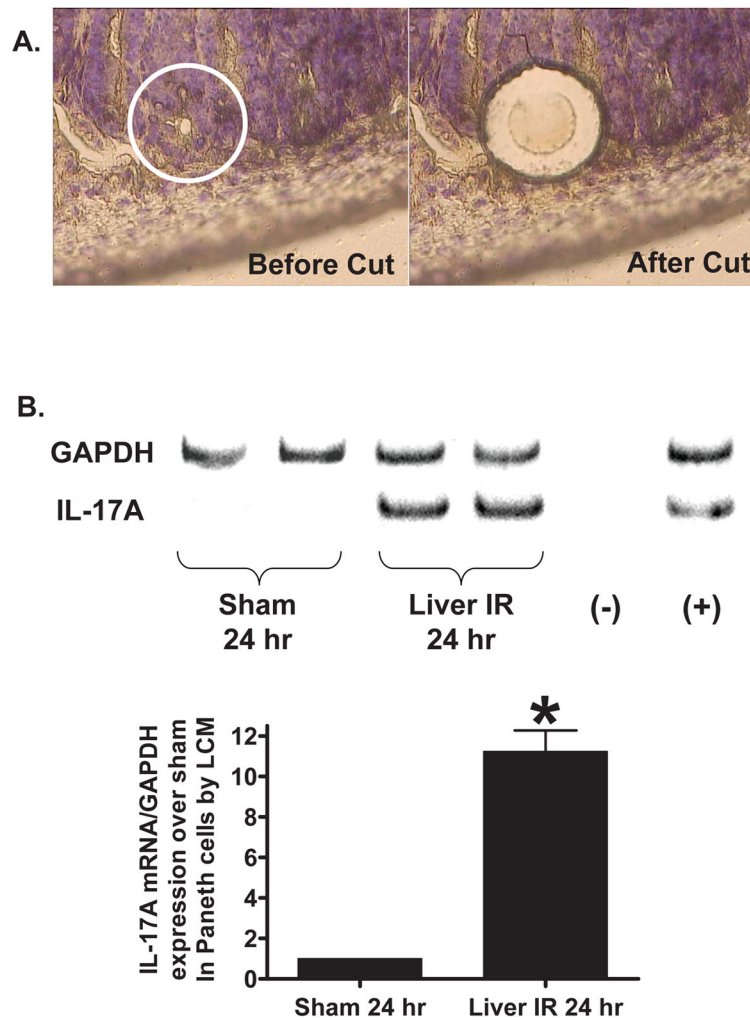


Figure 2.

A. Mouse small intestine (ileum) Paneth cells before (left) and after (right) laser capture micro-dissection (400X magnification). B. Representative RT-PCR analysis (top) and band intensity quantifications (bottom) for IL-17A mRNA extracted from Paneth cells with laser capture micro-dissection. Hepatic IR caused increased IL-17 transcripts in these cells (representative of 4 experiments). (-) negative control water blank. (+) positive control RT-PCR reaction. * $P < 0.05$ vs. sham-operated mice. Error bars represent 1 SEM.

Figure 3A 60 min liver ischemia and reperfusion

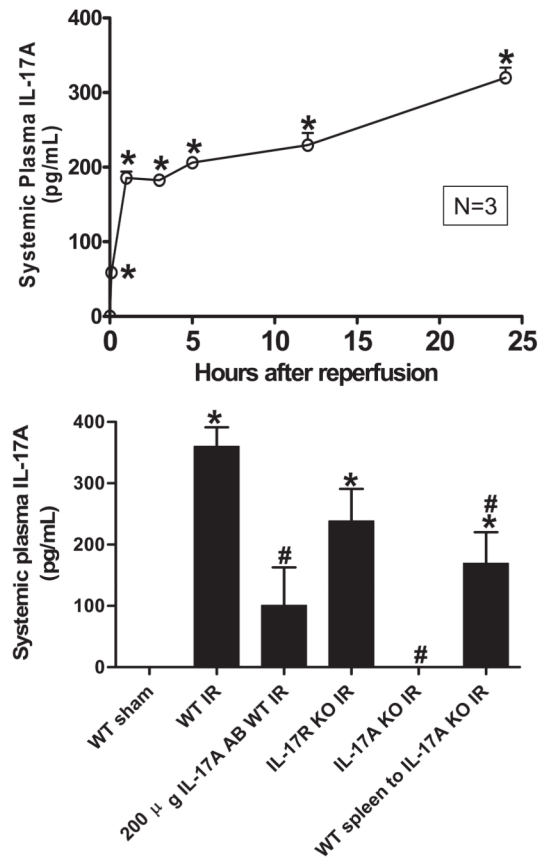


Figure 3B

60 min liver ischemia and 24 hr reperfusion

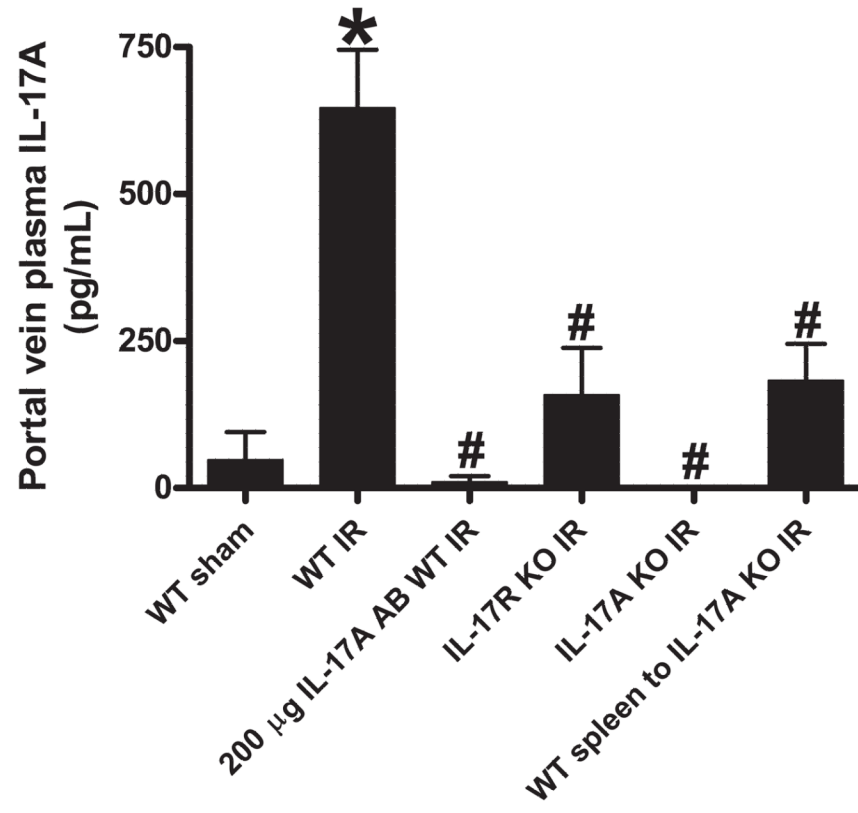
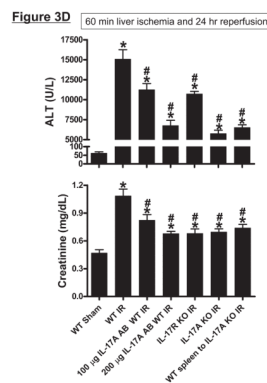
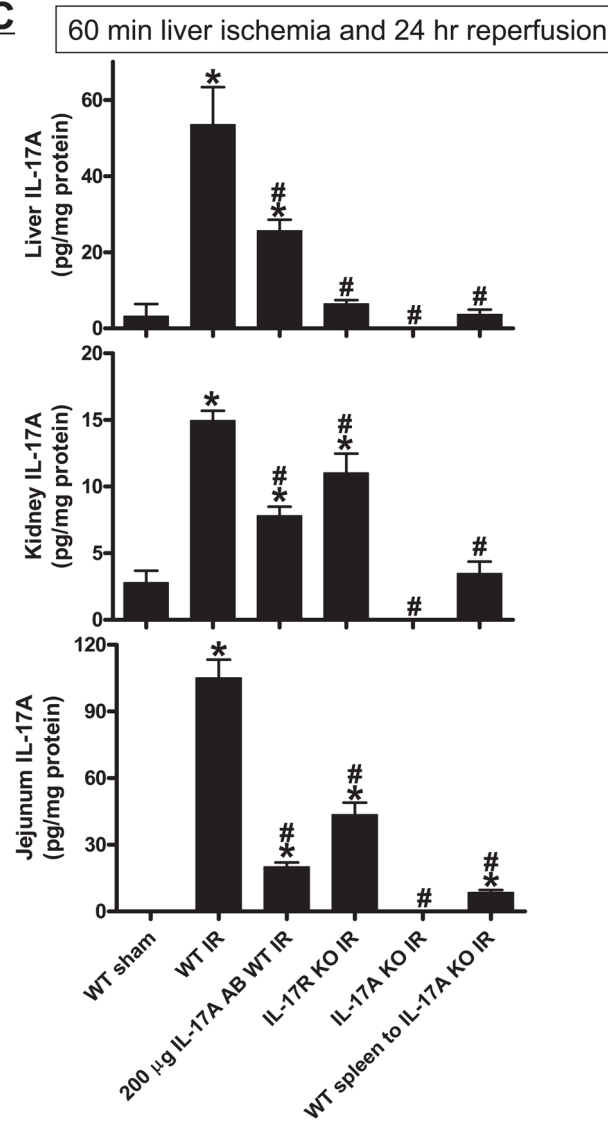


Figure 3C**Figure 3.**

Systemic (A) and portal plasma IL-17A levels (B), liver, kidney and small intestine (jejunum) IL-17A levels (C) and indices of hepatic (ALT) and renal (creatinine) injury (D) from mice subjected to sham-operation (Sham, N=4) or 60 min. hepatic ischemia and

reperfusion (IR, N=6). Sixty min. liver IR resulted in rapid increases in plasma IL-17A levels in mice (N=3, A). Neutralization of IL-17A (IL-17A AB, 100 or 200 μ g iv, N=5 each), deficiency in IL-17A receptor (IL-17R KO, N=5) or IL-17A (IL-17A KO, N=5) reduced plasma and tissue IL-17A levels and protected against hepatic and renal injury 24 hr after 60 min. hepatic IR compared to WT mice. IL-17A deficient mice (N=5) transfused with wild type splenocytes (Wild type spleen to IL-17A KO) also had significantly lower plasma and tissue IL-17A levels and were also protected against liver and kidney injury 24 hr after 60 min. hepatic IR. *P<0.05 vs. sham-operated mice. #P<0.05 vs. WT mice subjected to hepatic IR. Error bars represent 1 SEM.

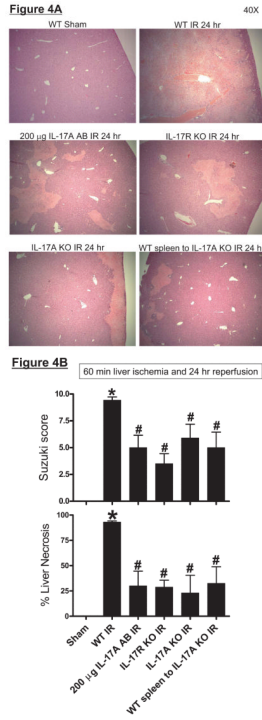


Figure 4. A. Representative photomicrographs (magnification 40X) of hematoxylin and eosin staining of the liver sections. Mice were subjected to sham-operation (sham, N=4) or to 60 min. hepatic ischemia followed by 24 hr reperfusion (IR, N=6). Necrotic hepatic tissue appears as light pink with inflammatory/vascular congestion. Photographs are representative of 4–6 independent experiments. Suzuki scores and percent liver necrosis (B) for livers from mice subjected to sham or hepatic IR. Neutralization of IL-17A (IL-17A AB, 200 µg iv), deficiency in IL-17A receptor (IL-17R KO) or IL-17A (IL-17A KO) significantly reduced liver necrosis 24 hr after 60 min. hepatic IR. IL-17A deficient mice transfused with wild type splenocytes are also protected against liver injury 24 hr after 60 min. hepatic IR. *P<0.05 vs. sham-operated mice. #P<0.05 vs. mice subjected to hepatic IR. Error bars represent 1 SEM.

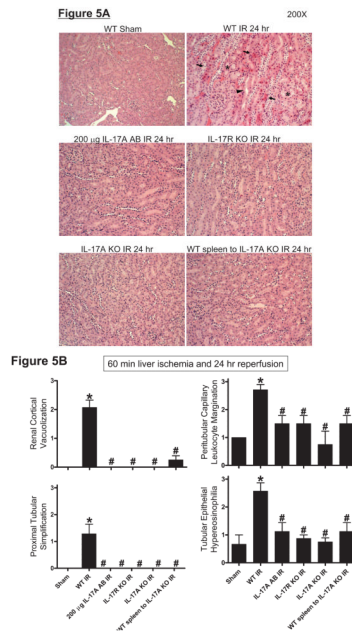


Figure 5.

A. Representative photomicrographs (magnification 200X) of hematoxylin and eosin staining of the kidney sections. Mice were subjected to sham-operation (sham, N=4) or to 60 min. hepatic ischemia followed by 24 hr reperfusion (IR, N=6). Sixty min. hepatic IR caused multifocal acute tubular injury including S3 segment proximal tubule necrosis (arrows), cortical tubular simplification (arrow head), cytoplasmic vacuolization (*). Photographs are representative of 4–6 independent experiments. B. Summary of renal injury scores (scale 0–3) for renal cortical vacuolization, peritubular leukocyte margination, proximal tubule simplification and renal tubular hypereosinophilia for kidney sections from mice subjected to sham or hepatic IR. Neutralization of IL-17A (IL-17A AB, 200 µg iv), deficiency in IL-17A receptor (IL-17R KO) or IL-17A (IL-17A KO) significantly reduces the renal injury 24 hr after 60 min. hepatic IR. IL-17A deficient mice transfused with wild type splenocytes are also protected against the renal injury 24 hr after 60 min. hepatic IR. *P<0.05 vs. sham-operated mice. #P<0.05 vs. mice subjected to hepatic IR. Error bars represent 1 SEM.

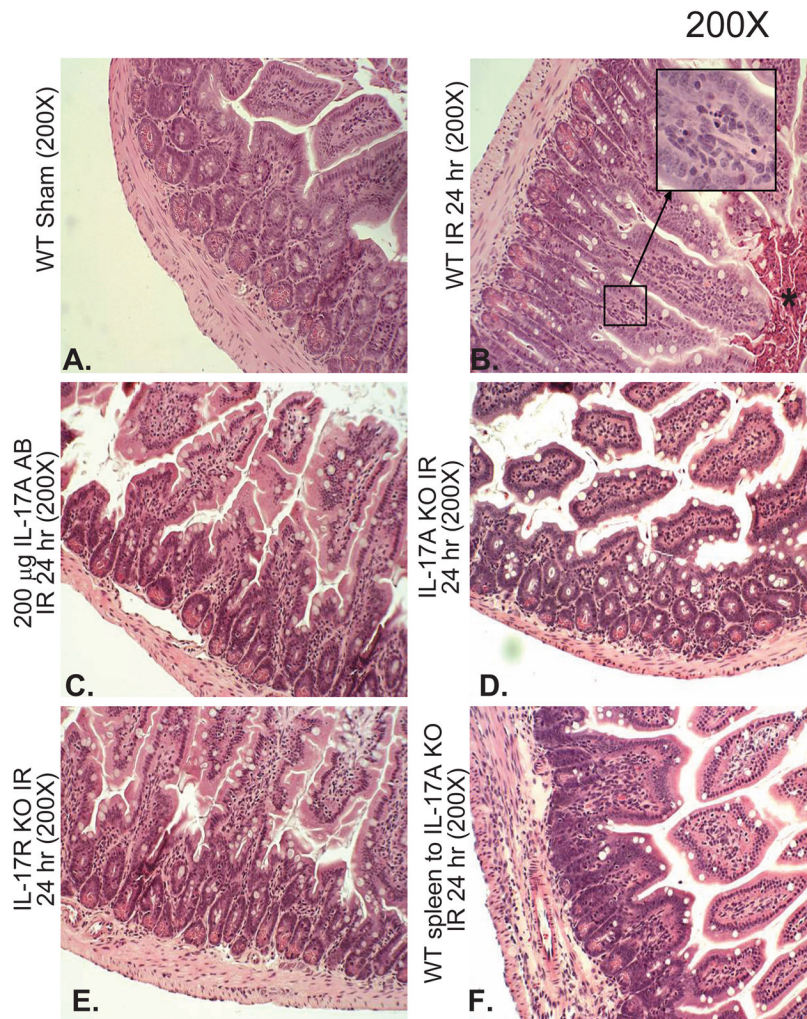


Figure 6.

A. Representative photomicrographs of small intestine from 4–6 experiments (hematoxylin and eosin staining, magnification 200X) of mice subjected to sham-operation (sham, N=4) or to 60 min. hepatic ischemia followed by 24 hr reperfusion (IR, N=6). Sham operated animals show normal-appearing intestine histology (A). In contrast, the small intestine sections from mice subjected to hepatic IR show villous endothelial cell apoptosis (magnified insert), severe epithelial cell necrosis of villous lining cells and the development of a necrotic epithelial pannus (*) over the mucosal surface compared to sham-operated animals (B). Neutralization of IL-17A (IL-17A AB, 200 µg iv, C), deficiency in IL-17A (IL-17S KO, D) or IL-17A receptor (IL-17R KO, E) significantly reduces the intestine injury 24 hr after 60 min. hepatic IR. IL-17A deficient mice transfused with wild type splenocytes are also protected against the intestine injury 24 hr after 60 min. hepatic IR (F).

Figure 7A

1000X

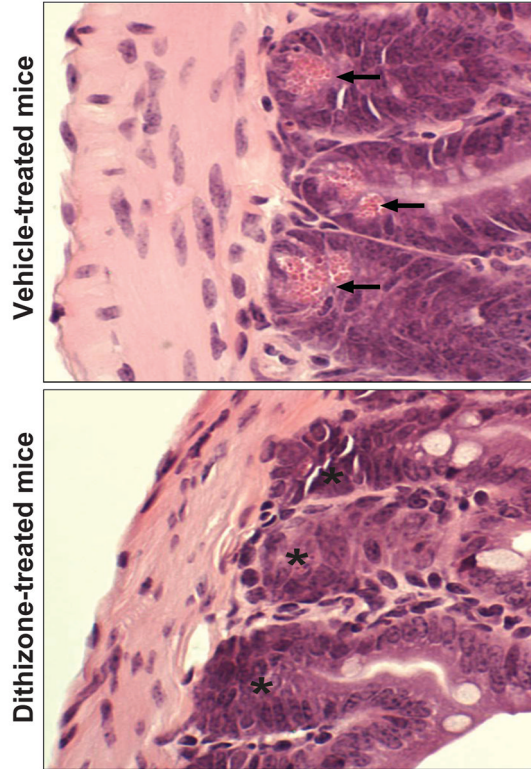
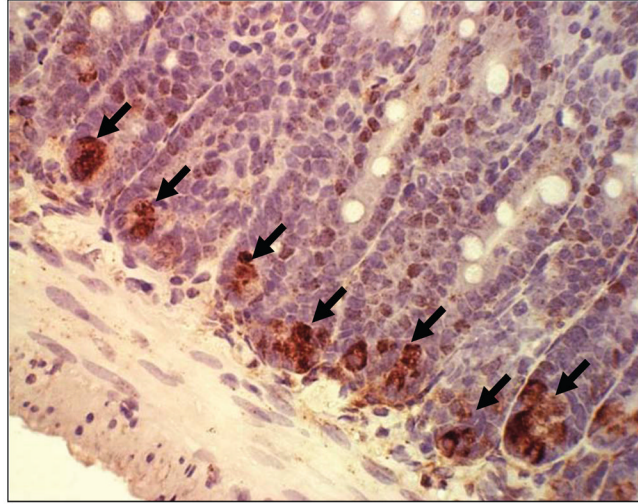


Figure 7B

400X

Vehicle-treated mice



Dithizone-treated mice

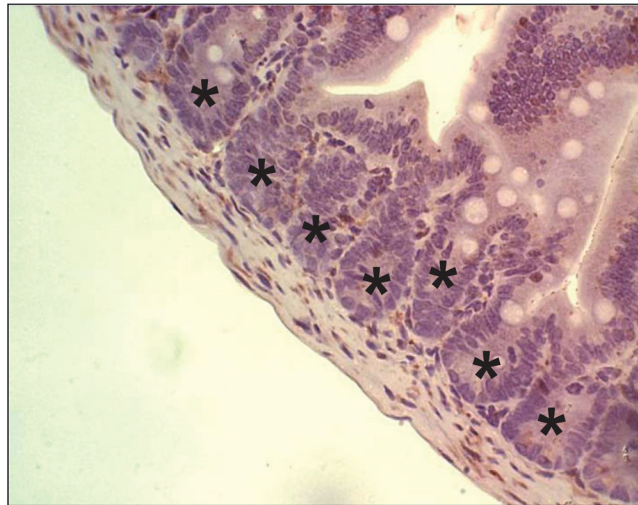
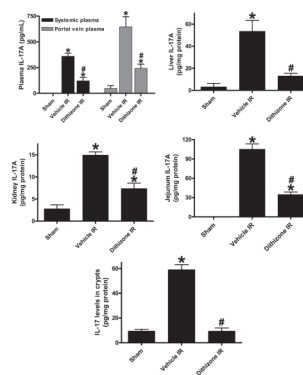


Figure 7C 60 min liver ischemia and 24 hr reperfusion



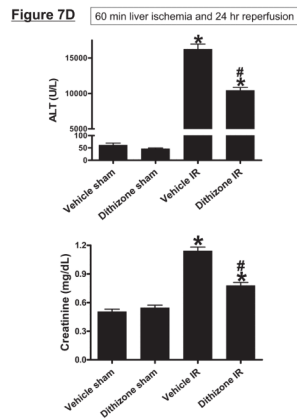


Figure 7.

A. Dithizone treatment depletes small intestinal Paneth cell granules (*). Representative (of 4 experiments) hematoxylin and eosin staining images of ileum from mice treated with vehicle (Li_2CO_3) or with dithizone 6 hr prior. Note near complete depletion of Paneth cell granules (arrows, magnification 1000X) after dithizone treatment (*). B. Representative (of 5 independent experiments, magnification 400X) images of lysozyme immunostaining in small intestine (ileum). Note that lysozyme stain was heavy in Paneth cells (arrows) of small intestinal crypts of mice treated with vehicle (Li_2CO_3). Paneth cell depletion with dithizone treatment eliminated lysozyme staining in Paneth cells (*). C. Dithizone treatment reduces plasma IL-17A levels in mice subjected to 60 min. hepatic IR (Dithizone IR, N=4). Dithizone treatment also reduced IL-17A protein upregulation in liver, kidney, small intestine and freshly isolated small intestinal crypts (N=4) 24 hr after 60 min. hepatic IR. D. Paneth cell granule depletion with dithizone treatment protects against hepatic (ALT) and renal (creatinine) injury after liver IR. Mice were subjected to sham-operation (Sham, N=4) or hepatic IR (N=6), and plasma was collected 24 hrs after reperfusion. * $P < 0.05$ vs. sham-operated mice. # $P < 0.05$ vs. vehicle treated mice subjected to hepatic IR. Error bars represent 1 SEM.

Figure 8A

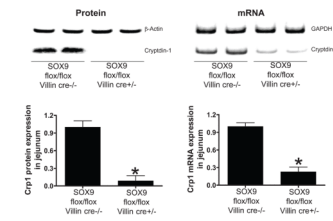


Figure 8B

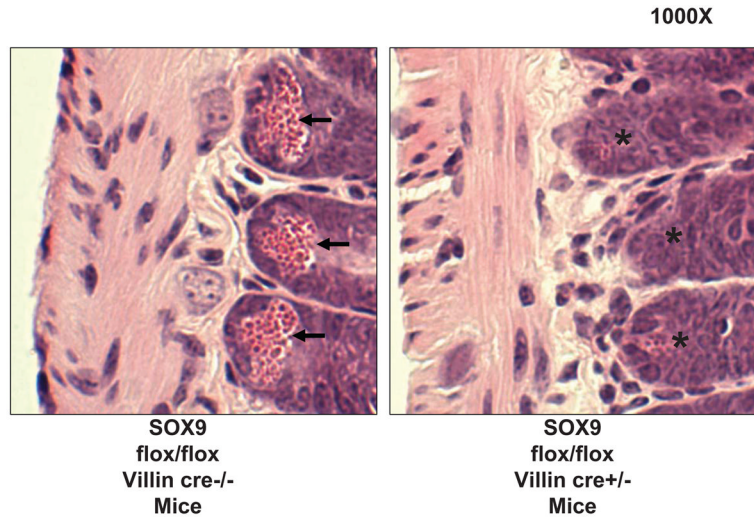


Figure 8C

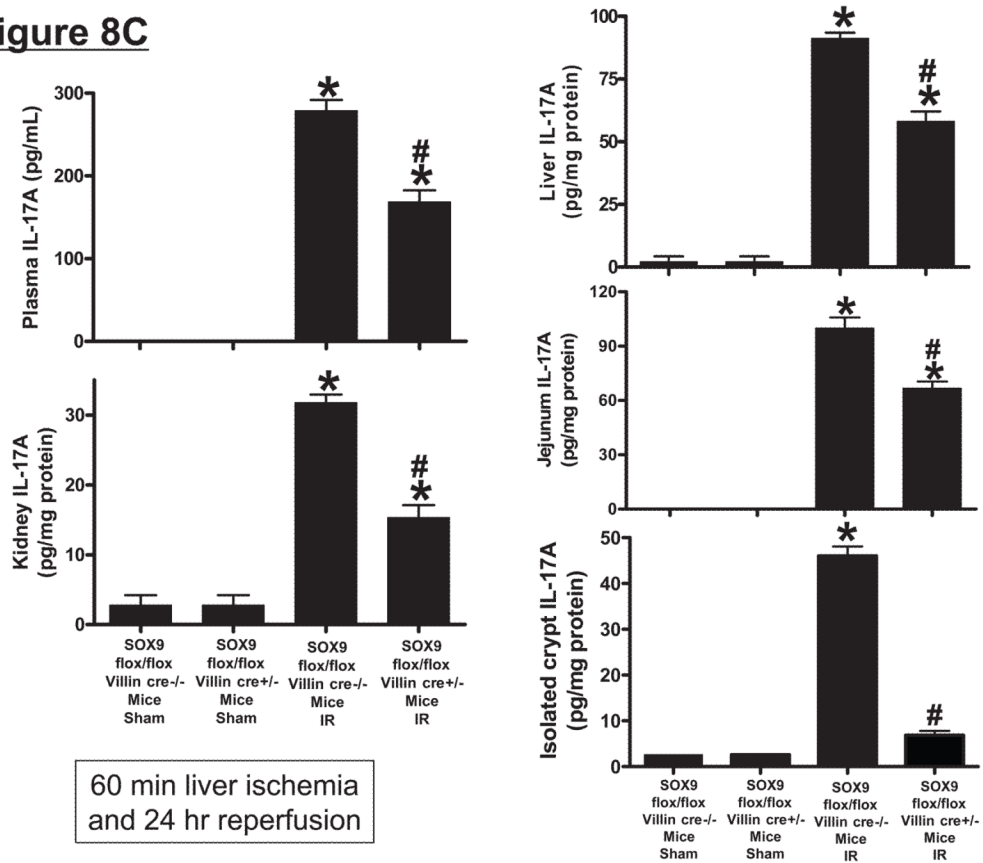
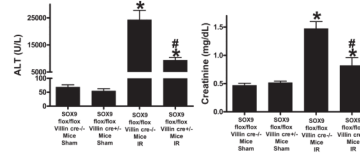


Figure 8D 60 min liver ischemia and 24 hr reperfusion

**Figure 8.**

SOX9 flox/flox Villin Cre^{+/-} (selective SOX9 deletion in intestinal epithelia) mice are deficient in Paneth cell marker (cryptdin-1 protein and mRNA, A) and in Paneth cells (B) compared to wild type (SOX9 flox/flox Villin Cre^{-/-}) mice. Figure 7B shows near complete deficiency of Paneth cells (indicated by arrows in SOX WT mice, magnification 1000X) in SOX9 flox/flox Villin Cre^{+/-} mice (*). C. Mice were subjected to sham-operation (Sham, N=4) or 60 min. hepatic IR (IR, N=4). Paneth cell deficiency in SOX9 flox/flox Villin Cre^{+/-} mice reduces plasma, liver, kidney, small intestine (jejunum shown) and freshly isolated small intestinal crypt IL-17A levels in mice subjected to 60 min. hepatic IR (N=4). D. Paneth cell deficiency in SOX9 flox/flox Villin Cre^{+/-} mice protects against hepatic (ALT) and renal (creatinine) injury compared with SOX9 flox/flox Villin Cre^{-/-} mice subjected 60 min. hepatic IR. *P<0.05 vs. sham-operated WT mice. #P<0.05 vs. WT mice subjected to hepatic IR. Error bars represent 1 SEM.